Dynamics of Energy Transfer by Singlet Excitons in Naphthalene Crystals as Studied by Time-Resolved Spectroscopy

H. Auweter *, A. Braun, U. Mayer, and D. Schmid

Physikalisches Institut, Teil 3, Universität Stuttgart

Z. Naturforsch. **34a**, 761–771 (1979); received April 5, 1979

The time-resolved sensitized fluorescence of anthracene-doped naphthalene crystals following picosecond-pulse excitation was investigated experimentally as a function of dopant concentration and temperature. The influence of the excitation intensity on the decay of pure naphthalene crystals is studied and yields an almost temperature-independent annihilation constant, $\gamma_{ss} \approx 4 \times 10^{-11}$ cm^3 s^{-1}. The analysis of the time-resolved host and guest fluorescence shows that the energy transfer rate, k_{HG}, changes its functional form with the guest concentration. The temperature dependence of the energy transfer rate is explained tentatively in terms of phonon relaxation and phonon promotion processes.

1. Introduction

One of the most promising ways to study energy transfer processes in the singlet state of molecular crystals is to investigate the time-resolved fluorescence of host and guest molecules in doped crystals. To our knowledge the first measurements of this type have been performed by Mansour and Weinreb using anthracene-doped naphthalene crystals [1]. Extensive studies on the same system as well as on a number of similar systems have been carried out by Powell and coworkers [2]. The result of their investigations was that the energy transfer shows an "anomalous" behaviour, which means that the observed time-resolved host and guest fluorescence cannot be interpreted in terms of a model which assumes a time-independent energy transfer rate. In the experiments of Powell and coworkers it was shown that the rate of energy transfer from the host crystal to the guest molecules following the creation of host excitons by a short light pulse depends on the time which has elapsed after the pulse. Powell and Soos have proposed a "generalized random walk model" in order to explain this observation [3, 4]. However, it is our opinion that a detailed understanding of the excitonic energy transfer, in particular of the nature of the exciton motion as well as of its interaction with a defect has not yet been achieved.

The aim of our investigations therefore is to study the kinetics of the energy transfer in different crystals with the largest possible range of dopant concentrations and in a wide range of temperature. We have performed these experiments by studying the time dependence of the sensitized fluorescence following a two-photon picosecond-pulse excitation. In this paper we report the experimental results which were obtained on naphthalene crystals doped with anthracene, in spite of the fact that it is still not possible to present a unified model for the energy transfer. We will therefore include only a few points which might be relevant for the explanation of the experimental observations. However, they should be considered merely as possible approaches to an understanding of the energy-transfer mechanism. To obtain a profound insight in this problem additional experiments on different systems with improved time resolution and sensitivity are required. Such experiments are currently under way.

2. Experimental

2.1. Experimental Set-up

The measurement of the time-resolved fluorescence is in principle a straight-forward experiment: the crystals are excited to some vibronic level of the first excited singlet state (S_1) with an ultrashort light pulse and the subsequent temporal behaviour of the host and guest fluorescence is measured. Figure 1 shows the basic set-up.

The ultrashort light pulses were produced in a mode-locked dye laser (model SUA 33, Electro Photonics). The active medium was a 2×10^{-4} molar

* Present address: Department of Chemistry, University of California, Berkeley, California 94720, USA.

Reprint requests to Prof. D. Schmid, Physikalisches Institut, Teil 3, Universität Stuttgart, Pfaffenwaldring 57, D-7000 Stuttgart 80, Germany.

0340-4811 / 79 / 0600-0761 $ 01.00/0

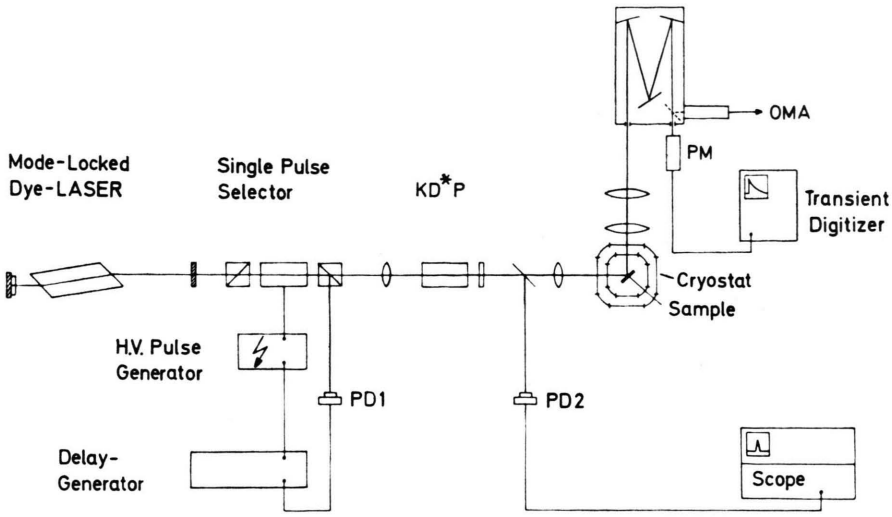

Fig. 1. Basic experimental set-up for the time-resolved measurement of sensitized fluorescence. See text for a detailed description.

solution of rhodamine 6G in water or methanol. A 5×10^{-5} molar solution of DODCI in methanol was used as mode-locking dye. The pulse trains consisted of roughly 400 pulses, the individual pulses being separated by about 5 ns. Single pulses were selected from the early part of the pulse trains, i.e. before the pulses reached their maximum intensity in order to obtain clean pulses with a narrow spectral bandwidth and a short pulse duration. The pulse selector consisted of two crossed Glan-Taylor prisms and a Pockels cell. Once a pulse of the early part of the train reached a threshold energy a delay pulse generator (model 438, Cordin) was triggered by means of the photodiode PD 1 (UVHC 20, Valvo). After the appropriate period of time this delay generator fired a pregated krytron circuit. The output was applied to the Pockels cell via a pulse-shaping Blumlein network. In this way it was possible to select any arbitrary pulse from the pulse train.

The pulse duration was measured with the two-photon fluorescence (TPF) method [5] using a saturated solution of dimethyl-POPOP in benzene as fluorescing dye. The fluorescence at 4300 Å was observed with a SIT-OMA-detector head (model 1205 D, PAR). From these experiments the pulse halfwidth was determined to be (7 ± 3) ps.

The pulse energy of each single pulse was monitored with the vacuum photodiode PD 2 (HSD 1850 M 20 UVS, ITL), which had been calibrated using a pyroelectric detector (J 3-02, Molectron) as a reference. The energy of a single pulse was typically a few μJ at 6050 Å and after being frequency doubled by a KD*P-crystal the typical pulse energy was about 0.5 μJ at 3025 Å.

The samples were mounted in a home-made continuous-flow cryostate. The accessible range of temperature was between 3.8 K and 300 K. The temperature stability was better than ± 0.02 K at low temperatures and better than ± 0.5 K above 100 K.

The luminescence of the samples was spectrally resolved with a 0.6 m monochromator (HRP, Jobin Yvon). The time-resolved fluorescence was recorded using a fast photomultiplier (C 31024, RCA). The signals were finally recorded using either a 500 MHz oscilloscope (model 7904, Tektronix) or a transient digitizer (model R 7912, Tektronix). The overall risetime of the system was less than 1 ns.

2.2. Crystals

The experiments were performed using both pure and anthracene-doped naphthalene crystals. They were grown by the Stuttgarter Kristallabor using the Bridgman method. The starting material was commercially available naphthalene, which had been purified carefully by applying the following procedure: chromatographic purification (Al_2O_3), zone refinement (200 passages), fusion with potassium, zone refinement (200 passages). No impurities were detectable spectroscopically in the undoped crystals grown from this material. This implies that

the residual concentration of, for instance, 2-methylnaphthalene was less than 10^{-8} mole/mole ($<5\times10^{13}$ cm^{-3}).

For the doped crystals zone-refined anthracene was added to the melt at concentrations between 1×10^{-2} and 3×10^{-5} mole anthracene/mole naphthalene. The resulting relative guest concentration in the crystal, c_G, varied between 4×10^{-7} and 4×10^{-5} mole/mole (corresponding to 2.2×10^{15} cm$^{-3}\lesssim N_G\lesssim 2.2\times10^{17}$ cm^{-3}, where N_G is the number of guest molecules per cm^{-3}).

The actual guest concentration for each sample was determined in situ by measuring the quantum flux ratio, Q_G/Q_H, as described by Hammer [6] and Zibold [7]. For this purpose the crystals could be illuminated with light from a mercury high-pressure lamp which was passed through an appropriate filter combination. The resulting steady state fluorescence spectra were recorded using a standard photomultiplier (6256, EMI). For the sake of clearness this auxiliary equipment was omitted in Figure 1.

Examples for spectra obtained in this way are shown in Fig. 2 for $T=300$ K and $T=5$ K, respectively. It was established in Ref. [6] and [7] that the anthracene (guest) concentration, c_G, can be determined from the ratio of the quantum flux Q_G/Q_H of the guest and the host fluorescence using the following relations:

$$\log(Q_G/Q_H) = 1{,}2\log c_G + 7 \quad (1)$$

and

$$\log(Q_G/Q_H) = 0{,}7\log c_G + 3{,}5 \quad (2)$$

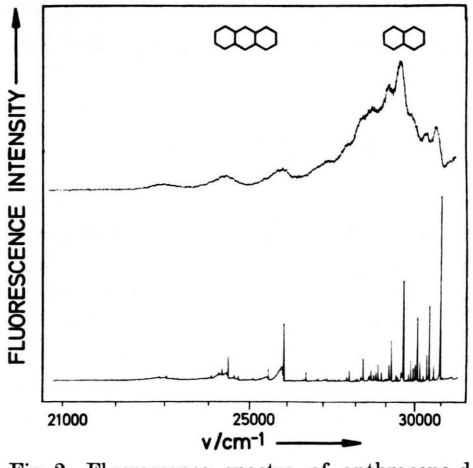

Fig. 2. Fluorescence spectra of anthracene-doped naphthalene at 300 K (top) and at 5 K (bottom). Guest concentration $c_G = 6\times10^{-7}$ mole anthracene/mole naphthalene (3.3×10^{15} cm^{-3}).

for $T=5$ K [6] and $T=300$ K [7], respectively. The concentrations quoted in this work were always determined on the particular sample under consideration using these relations. It was estimated that the absolute values of the concentrations are accurate at least within a factor of 2, whereas the relative accuracy is better than $\pm30\%$. Since the anthracene concentration varies within a sample, the orientation and the imaging of the samples onto the monochromator were not changed, once the doping concentration had been determined.

There are limits to the usable dopant concentrations: The lower limit of $c_G\approx4\times10^{-7}$ mole/mole (2.2×10^{15} cm^{-3}) is due to the fact that for smaller c_G the guest fluorescence is to weak to be detected in the time-resolved experiment. The upper limit — $c_G\approx3\times10^{-5}$ mole/mole (1.7×10^{17} cm^{-3}) — is given by the restricted ability of the anthracene molecule to be built in substitutionally. Therefore, the anthracene concentration could only be varied by about two orders of magnitude.

The crystals were cleaved in the crystallographic ab-plane. The samples had a size of about $(5\times5\times1)$ mm^3. The crystals were oriented and the crystallographic quality was checked by means of a polarizing microscope. The samples were attached to the sample holder without strain, the *E*-vector of the incident light pulse being parallel to either the *a*- or the *b*-axis.

3. Experimental Results: Singlet-Exciton Interaction in Pure Naphthalene

Figure 3 presents fluorescence decay curves obtained from a pure naphthalene crystal at 50 K following excitation into a vibronic level of the S_1 state 33058 cm^{-1} above the ground state S_0 using single ultrashort light pulses. The upper curve (a) was obtained with low excitation density (initial exciton density at $t=0$: $n_0\approx9.7\times10^{14}$ cm^{-3}), which was achieved by two-photon excitation as described in the next section. The lower curve (b) was recorded following high excitation density ($n_0\approx2.4\times10^{17}$ cm^{-3}) obtained with one-photon absorption. There are marked differences between the two curves. Whereas curve a is monoexponential with a decay time $\tau_H^0=119$ ns, curve b decays more rapidly in the early part with a nonexponential characteristic.

This observation can be explained using the concept of mutual annihilation of two singlet

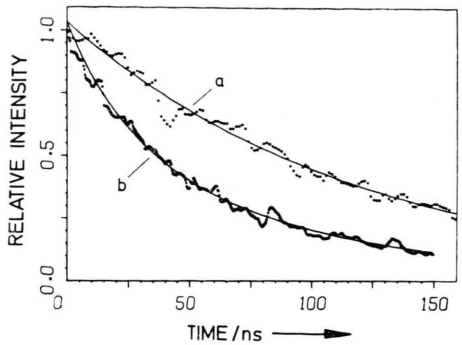

Fig. 3. Fluorescence decay of a pure naphthalene crystal observed at 29578 cm^{-1} [0,0 − (512 + 1386) cm^{-1}] and at $T = 50$ K.
a) Initial exciton density $n_0 = 9.7 \times 10^{14}$ cm^{-3}. Exponential decay with $\tau_H{}^0 = 119$ ns.
b) Initial exciton density $n_0 = 2.4 \times 10^{17}$ cm^{-3}. Decay calculated according to Eq. (4) with $\gamma_{ss} = 5.5 \times 10^{-11}$ cm^3/s and $\tau_H{}^0 = 119$ ns.

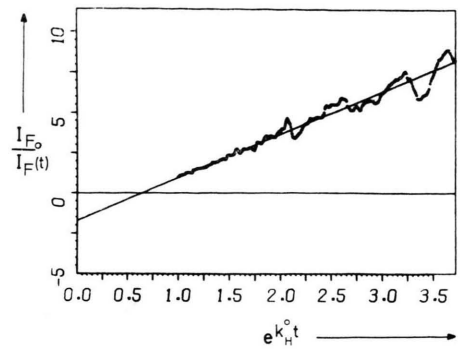

Fig. 4. Reciprocal of the fluorescence intensity, $1/I_F(t)$, normalized to the initial intensity I_{F0} as a function of $\exp(k_H{}^0 t)$ for $T = 50$ K and $n_0 = 2.4 \times 10^{17}$ cm^{-3} (curve b of Figure 3).

excitons by an Auger-type autoionization process and successive nonradiative decay, which occurs at sufficiently high exciton densities [8—12]. The time dependence of the exciton concentration $n_H(t)$ following an excitation pulse $G(t)$, which in our case can be approximated by a δ-function, is governed by the following rate equation:

$$dn_H/dt = G(t) - k_H^0 n_H - \gamma_{ss} n_H^2 , \qquad (3)$$

where γ_{ss} is the singlet-singlet annihilation rate constant, which accounts for the bimolecular decay process. For a δ-function excitation the solution of Eq. (3) is given by

$$n_H(t) = \frac{n_0 \exp(-k_H^0 t)}{(\gamma_{ss} n_0/k_H^0)[1 - \exp(-k_H^0 t)] + 1} . \qquad (4)$$

Equation (4) can be rewritten to yield

$$n_0/n_H(t) = [\gamma_{ss} n_0/k_H^0 + 1] \exp(k_H^0 t) - \gamma_{ss} n_0/k_H^0 . \qquad (5)$$

n_0 is the initial exciton density, which exists immediately after the pump pulse. The fluorescence intensity $I_F(t)$ is related to the exciton density by the proportionality $I_F(t) \propto k^* \cdot n_H(t)$, where k^* is the radiative decay rate constant. Therefore, if we plot $I_{F0}/I_F(t)$ as a function of $\exp(k_H^0 t)$, we expect a straight line, the slope of which as well as the ordinate intercept yield γ_{ss} independently, provided n_0 and k_H^0 are known accurately enough. (I_{F0} is the initial fluorescence intensity.) Figure 4 confirms this prediction. k_H^0 is obtained from the low-exciton-density decay curve (curve a in Figure 3): $k_H^0 = 8.4 \times 10^6$ s^{-1}. The most critical problem in obtaining γ_{ss} is the estimate of n_0. In deriving Eq. 5 it has been assumed that n_0 is homogeneous. In the experiment this postulate is severely violated because of two reasons: Firstly, the absorption coefficient of naphthalene at 3025 Å is very high (roughly 6000 cm^{-1}) [13, 14]. Therefore, with increasing penetration depth, the initial exciton density decreases rapidly due to Beer's law.

Secondly, in order to obtain a high exciton density the laser light was focused into a small spot on the crystal surface. The size of this spot could be measured quite accurately using an optical multichannel analyzer (model 1205, PAR). The excitation intensities across this spot were, of course, quite nonuniform, in particular if the size of the spot was very small. It is possible, in principle, to solve Eq. (3) also for such inhomogeneous excitations [11]. However, it was felt that the available experimental data are not yet accurate enough to make such an evaluation meaningful. We therefore approximated n_0 by an average initial exciton density, which is defined by the total number of photons absorbed, divided by an average volume (effective spot size times penetration depth of the 33058 cm^{-1} photons) and we restricted the spot area to values above 1 mm^2. Of course, this approximation may cause large errors and it was estimated that the absolute values of γ_{ss} obtained in this way may be inaccurate by as much as a factor of 5. However, the relative error, for instance in the determination of the temperature dependence of γ_{ss} given in Fig. 5, is estimated to be less than $\pm 40\%$. Thus we conlcude that γ_{ss} depends only weakly on the temperature, but for an accurate

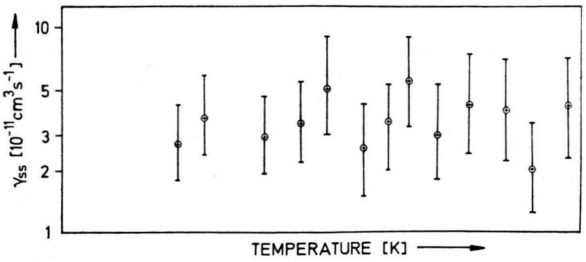

Fig. 5. Singlet-singlet annihilation rate constant γ_{ss} as a function of temperature.

determination of its absolute value additional experiments at improved sensitivity and temporal resolution are required. Such experiments are currently in preparation.

The fact that γ_{ss} changes only slightly with temperature suggests that exciton-phonon collisions, which occur during the exciton's migration and which scatter the excitons to different k-states within the band, do not strongly reduce the probability for encountering each other and for mutual annihilation.

To illustrate γ_{ss} one can define a critical exciton density n_c above of which the bimolecular decay exceeds the monomolecular decay. This quantity is defined by $k_H^0 = \gamma_{ss} n_c$. From Fig. 5 one obtains roughly $n_c \approx 2 \times 10^{17}$ cm^{-3}, regardless of the temperature within the experimental limits of error.

Several authors [2, 11, 15] have proposed explanations for γ_{ss} based on an exciton diffusion model. On the other hand, there is no conclusive evidence that singlet exciton move according to a diffusion process [16]. Furthermore, for an attempt to derive a diffusion constant from γ_{ss} it is necessary to make assumptions about the interaction radius. Therefore, in this work, we refrain from attempting such a derivation.

4. Dynamics of the Sensitized Fluorescence in the Guest-Host-System Anthracene in Naphthalene

4.1. Two-Photon Excitation

In order to avoid exciton-exciton annihilation and to achieve a homogeneous initial exciton distribution, all the experiments on the time dependence of the sensitized fluorescence reported in the remaining part of this paper were performed using two-photon excitation. For this purpose the laser output at 6050 Å was used without frequency doubling prior to its irradiation onto the crystal. Due to the selection rule for two-photon processes the S_1 state of naphthalene ($^1B_{2u}$) cannot be excited directly from the S_0 ground state (^1A_g) via a two-photon transition. An investigation of the polarized two-photon absorption spectra [17] has shown that the S_1 state in naphthalene crystals can be excited with photons of 6050 Å wavelength (16529 cm^{-1}), since in the region of twice their energy there are vibronic states of b_{2u} symmetry which are coupled to the electronic S_1-state.

The two-photon absorption cross section $\sigma^{(2)}$ for these photons in naphthalene is given by $\sigma^{(2)} = 10^{-50}$ cm^4 s · I, where I is the incident photon flux [18—20]. In our experiments I had a maximum value of roughly 10^{27} cm^{-2} s^{-1}, which yields a two-photon absorption coefficient of $\alpha^{(2)} \approx 0.05$ cm^{-1}. Thus two-photon excitation yields a uniform bulk excitation at a maximum exciton density of about 10^{15} cm^{-3} which assures that exciton-exciton annihilation is negligible.

Due to the relatively strong two-photon absorption of pure or doped naphthalene crystals the situation is somewhat different from the case of tetracene-doped anthracene, where two-photon absorption of the tetracene (guest) molecules and subsequent energy transfer from the higher excited guest molecules to the anthracene (host) crystal has been reported [20].

The results of fluorescence decay measurements following two-photon excitation of pure naphthalene have been published previously [12]. The observed decay characteristics were purely exponential above 15 K. In Fig. 6 the observed decay times are plotted as a function of temperature. For comparison the full

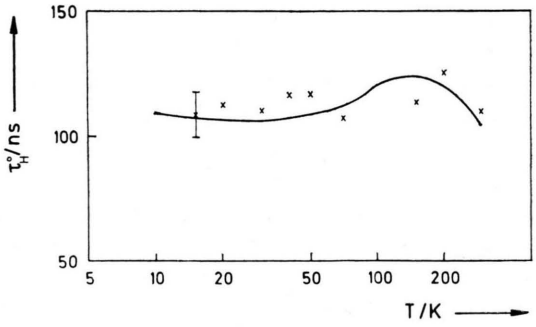

Fig. 6. Fluorescence decay time, τ_H^0, of a pure naphthalene crystal following two-photon excitation as a function of temperature. The full line indicates the observed temperature dependence, if low-intensity one-photon excitation was used.

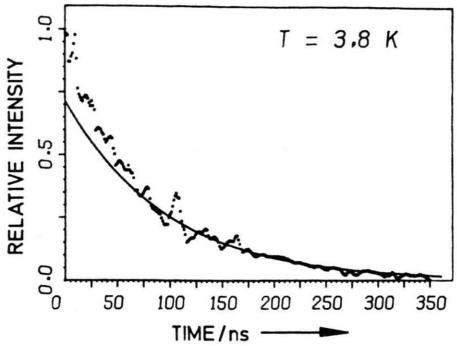

Fig. 7. Fluorescence decay of a pure naphthalene crystal following two-photon excitation at $T = 3.8$ K. The slight deviations from a purely exponential decay (full line, $\tau_H{}^0 = 100$ ns) in the early part of the decay are tentatively attributed to the presence of unavoidable shallow traps.

line indicates the decay times as determined using one-photon excitation at low excitation intensities [21, 22]. Within the limits of error ($\pm 10\%$ for two-photon excitation and $\pm 3\%$ for one-photon excitation, respectively) the two techniques yield identical decay times, which are almost independent of the temperature.

Only at temperatures below 15 K slight deviations from the exponential decay characteristic are observed (as illustrated by Figure 7). The initially faster decay, which varies for different samples is tentatively assigned to some unknown nonradiative shallow traps which provide an additional decay channel.

4.2. Host-Fluorescence Decay in Doped Crystals

The characteristics of the host-fluorescence decay in doped crystals depend on both the temperature and in particular on the dopant concentration. For samples in the range of high and medium dopant concentrations ($c_G > 5.4 \times 10^{-6}$ mole/mole $\triangleq 3 \times 10^{16}$ cm^{-3}) the observed decay characteristics were purely exponential within the limits of error in the entire accessible range of temperature. The reduction of the host fluorescence decay time was identical to that reported in previous publications [21, 22]. At lower concentrations the decay curves could not be fitted by a single exponential, the deviations being more pronounced the lower the concentration and the lower the temperature was. In the lowest-concentration sample (8.8×10^{-7} mole/mole $= 4.9 \times 10^{15}$ cm^{-3}) significant deviations from the monoexponential decay were observed at temperatures below 150 K, whereas for 5.2×10^{-6} mole/mole (2.9×10^{16} cm^{-3}) this was the case only below 7 K. These deviations will be discussed in Section 4.4. Since the deviations from an exponential decay are not very obvious, we focus our attention on the time dependence of the guest fluorescence, where the effects are less subtle. However, it should be emphasized that the time dependencies of the host fluorescence, which are predicted, if the parameters obtained from the guest fluorescence are used, are in full agreement with the experimental curves. Figure 8 illustrates the dependence of the host fluorescence decay on the dopant concentration for $T = 30$ K. The full lines were calculated using the parameters obtained from the guest fluorescence after applying the fitting procedure described in Section 4.4.

The decay times of the monoexponential curves and in particular their temperature dependencies agree well with those obtained previously with low-intensity one-photon excitation [21, 22]. However, when using one-photon excitation a biexponential decay was observed in highly doped samples ($c_G > 8 \times 10^{-6}$ mole/mole $\triangleq 4.5 \cdot 10^{16}$ cm^{-3}) at temperatures below 60 K. Tentatively, the initially faster decay has been attributed to unidentified shallow traps which were introduced by the high dopant concentration and which quench the exciton fluorescence partly. It was not observed in the current experiments, because the sensitivity in the two-photon excitation experiments is too low to allow the detection of the host fluorescence in the highly doped samples at low temperatures.

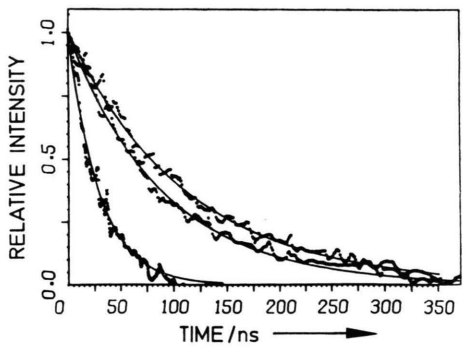

Fig. 8. Host fluorescence decay at $T = 30$ K as a function of dopant concentration. Upper curve: Pure crystal, $\tau_H = 112$ ns, center curve: Guest concentration $c_G = 1.1 \times 10^{-6}$ mole/mole (6.2×10^{15} cm^{-3}); $\tau_H = 90$ ns, lower curve: Guest concentration $c_G = 5.2 \times 10^{-6}$ mole/mole (2.9×10^{16} cm^{-3}); $\tau_H = 29$ ns.

4.3. Time-Resolved Guest Fluorescence

Whereas the deviations of the host fluorescence from the exponential characteristic are minor and there is little additional information compared to the previous results, the time dependence of the guest fluorescence yields important new aspects. Figure 9 presents a compilation of representative time-resolved guest fluorescence curves for low, medium and high dopant concentrations at various temperatures (5 K, 30 K, 100 K and 300 K). These curves were obtained by monitoring the time dependence of the 0,0-fluorescence band of anthracene (3868 Å ≙ 25856 cm^{-1}) following a two-photon excitation of the host crystal. They show a very characteristic change with temperature for all doping concentrations: at low temperatures the rise of the guest fluorescence is faster than at high temperatures and the maximum is reached more rapidly. Figure 10 gives an example for this in an enlarged scale for a dopant concentration of

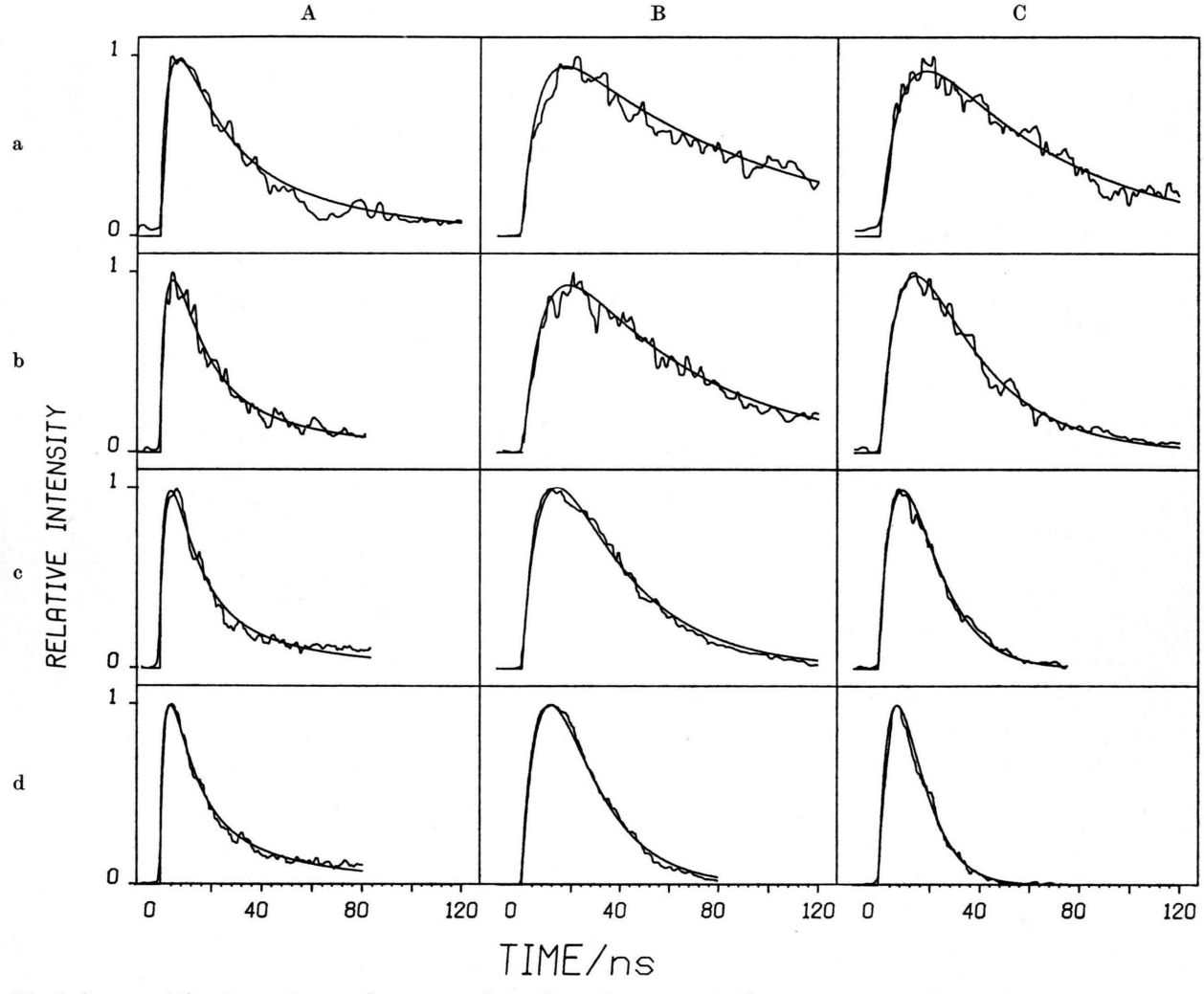

Fig. 9. Survey of the observed guest fluorescence decay for various concentrations.
From left to right: A) $c_G = 8.8 \times 10^{-7}$ mole/mole (4.9×10^{15} cm^{-3});
B) $c_G = 5.2 \times 10^{-6}$ mole/mole (2.9×10^{16} cm^{-3});
C) $c_G = 3.8 \times 10^{-5}$ mole/mole (2.1×10^{17} cm^{-3}).
From top to bottom: a) $T = 300$ K; b) $T = 100$ K; c) $T = 30$ K; d) $T = 5$ K. The full lines are calculated using the fitting procedure described in Section 4.4. For $c_G = 8.8 \times 10^{-7}$ mole/mole the guest fluorescence at room temperature was too weak to be analyzed. Therefore the curve obtained at 150 K is shown in this case.

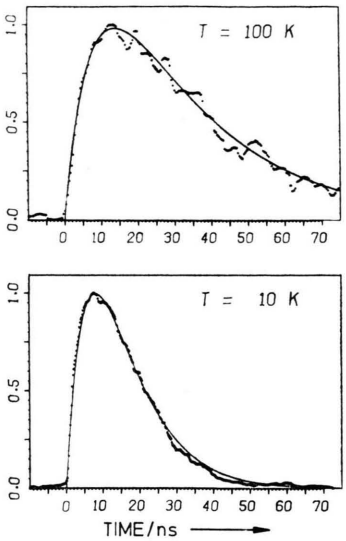

Fig. 10. Guest fluorescence at 100 K and 10 K for $c_G = 3.8 \times 10^{-5}$ mole/mole (2.1×10^{17} cm^{-3}). With decreasing temperature the rise of the guest fluorescence becomes faster ($t_{max} = 14.3$ ns and 7.8 ns for 100 K and 10 K, respectively.

3.8×10^{-5} mole/mole (2.1×10^{17} cm^{-3}). At $T = 100$ K the maximum is reached after $t_{max} = 14.3$ ns, whereas at $T = 10$ K the rise is much faster and the maximum is already observed 7.8 ns after excitation. The decay of the guest fluorescence at low

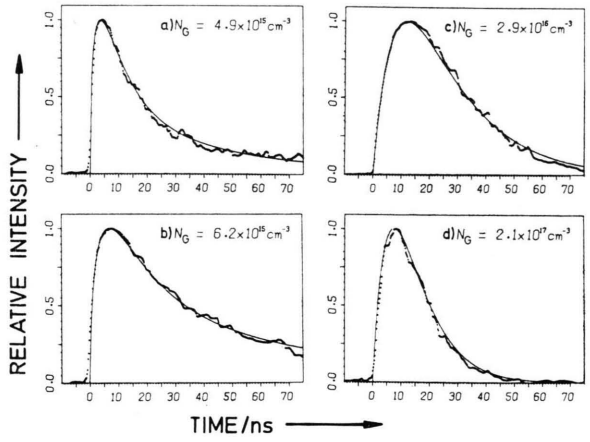

Fig. 11. Time resolved guest fluorescence observed at 3868 Å (25 856 cm^{-1} = 0,0) at 5 K as a function of dopant concentration.

a) $c_G = 3.8 \times 10^{-5}$ mole/mole (2.1×10^{17} cm^{-3}), $t_{max} = 7.8$ ns;
b) $c_G = 5.2 \times 10^{-6}$ mole/mole (2.9×10^{16} cm^{-3}), $t_{max} = 12.0$ ns;
c) $c_G = 1.1 \times 10^{-6}$ mole/mole (6.2×10^{15} cm^{-3}), $t_{max} = 7.3$ ns;
d) $c_G = 8.8 \times 10^{-7}$ mole/mole (4.9×10^{15} cm^{-3}), $t_{max} = 4.0$ ns.

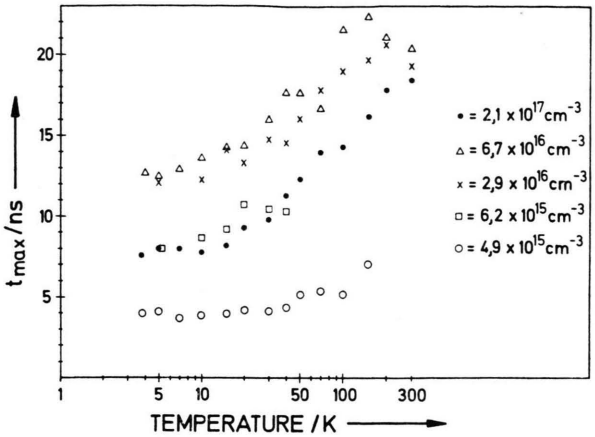

Fig. 12. Time t_{max}, after which the guest fluorescence reaches its maximum for various guest concentrations as a function of temperature.

temperatures is also faster than at high temperatures. The full lines in Figs. 9, 10 and 11 were calculated using the fitting procedure given in Section 4.4.

The most striking phenomenon is the observed concentration dependence of t_{max} (see Figs. 11 and 12). It has its minimum value for the lowest concentration ($c_G = 8.8 \times 10^{-7}$ mole/mole $= 4.9 \times 10^{15}$ cm^{-3}) although the average distance which an exciton must migrate to reach a guest is relatively large. If the concentration is increased to about 1.2×10^{-5} mole/mole (6.7×10^{16} cm^{-3}), t_{max} increases roughly by a factor of 3. Following a further increase of the dopant concentration to 3.8×10^{-5} mole/mole a decrease of t_{max} of about 30% is observed. An attempt to discuss this phenomenon is presented in the next section.

4.4. Discussion

The concentration dependence of t_{max} gives a strong indication that it is not appropriate to assume that the energy transfer to the guest molecules is governed by an energy transfer rate which is simply proportional to the concentration. In order to obtain information about the transfer process we have attempted to fit our experimental curves with theoretical curves which are based on the concept introduced by Powell and coworkers [2]. They have tackled the problem of explaining the time dependence of the guest fluorescence by introducing a time-dependent energy transfer rate, which they based on a so-called generalized random walk model [4]. The results of this model are

essentially equivalent with those of the diffusion theory [15, 23]. For an isotropic exciton motion in three dimensions they both predict a rate of energy transfer from the host to the guest, which is proportional to the guest concentration and which can be written as

$$k_{HG} = a + b\,t^{-1/2}\,, \tag{6}$$

where a and b are parameters, which are proportional to the guest concentration and furthermore depend on the characteristic of the exciton motion and the "trapping capacity" of the guest molecule. Figure 13 illustrates the quantities which are necessary to set up the rate equations for the concentrations of excited host and guest molecules, n_H and n_G respectively, following an excitation $G(t)$:

$$dn_H/dt = G(t) - k_H^0\, n_H(t) - k_{HG}(t)\, n_H(t)\,, \tag{7}$$

$$dn_G/dt = -\,k_G^0\, n_G(t) + k_{HG}(t)\, n_H(t)\,. \tag{8}$$

k_H^0 and k_G^0 are the decay rate constants of the excited host and guest molecules. The solutions of Eqs. (7) and (8) for a transfer rate as given by Eq. (6) following a δ-function excitation term were obtained by Heber [24]. The full lines in Figs. 9—11 are optimum fittings of these solutions to the observed curves with a and b as adjustable parameters. The obtainable fitting is quite satisfactory. The resulting fitting parameters are also adequate to explain the observed host-fluorescence decay at corresponding experimental conditions. In this way the observed behaviour can be characterized by giving the values of the fitting parameters.

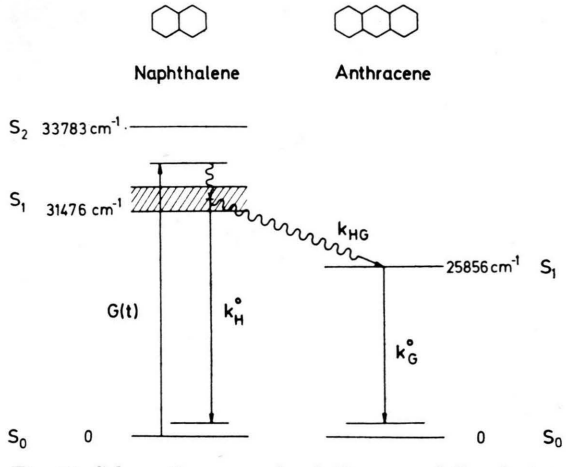

Fig. 13. Schematic energy level diagram of the electronic singlet state of anthracene-doped naphthalene. The relevant transitions involved in the experiments are indicated with their respective rates.

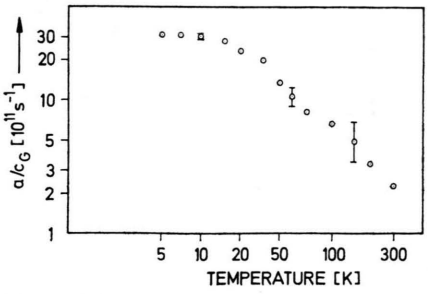

Fig. 14. Temperature dependence of the time independent part of the energy transfer rate in highly doped samples, $k_{HG}^0 = a/c_G$, in a double logarithmic scale.

The following qualitative behaviour was obtained: In the high-concentration samples ($c_G > 10^{-5}$ mole/mole $\triangleq 5.5 \times 10^{16}$ cm^{-3}) only parameter a is relevant, in the intermediate range of concentrations (10^{-5} mole/mole $> c_G > 1.1 \times 10^{-6}$ mole/mole or 5×10^{16} cm$^{-3} > N_G > 6 \times 10^{15}$ cm^{-3}) both terms, a and b, show up whereas in the low-concentration samples ($c_G < 1.1 \times 10^{-6}$ mole/mole $= 6 \times 10^{15}$ cm^{-3}) b dominates the energy transfer [12].

In the low-concentration samples b can be determined in the entire range of temperature between 4 K and 300 K. For the intermediate concentrations it was detectable only below 50 K. In both cases b was independent of the temperature within the rather large limits of error of about $\pm 60\%$.

According to the diffusion model b was expected to be proportional to the concentration. The experimental numbers, however, contradicted this prediction strongly: For $c_G = 8.8 \times 10^{-7}$ mole/mole (4.9×10^{15} cm^{-3}) the quantity b/c_G was obtained as 1.3×10^9 s$^{-1/2} \pm 60\%$; for $c_G = 5.2 \times 10^{-6}$ mole/mole (2.9×10^{16} cm^{-3}) it was almost 2 orders of magnitude smaller: $b/c_G \approx 2.0 \times 10^7$ s$^{-1/2}$.

The quantity a on the other hand is proportional to the concentration, within experimental error, as predicted by the diffusion model. In Fig. 14 we have plotted a/c_G as a function of the temperature in a double logarithmic scale. We denote this quantity as k_{HG}^0. The observed temperature dependence is identical with that reported in Ref. [22], where a time-independent energy transfer rate had been postulated to explain the experimental curves. There are several reasons why b did not show up in that work: Firstly, the doping of the samples was fairly high. Secondly, the host-fluorescence was studied predominantly in that work. This quantity, however, indicates the existence of a time-dependent part of k_{HG} much

less sensitively than the guest fluorescence. Finally, the time resolution was lower in Reference [22].

5. Conclusions

The most surprising result of this work is the strong concentration dependence of b/c_G. In Ref. [12] we tried to illustrate this on the basis of a diffusion model by extracting concentration-dependent diffusion constants and trapping radii. However, this should not lead to the assumption that the diffusion model yields a correct description of the energy transfer process. On the contrary, the concentration dependence of the trapping radii and the diffusion constants contradicts the usual concepts strongly. Many different approaches have been made to understand the energy transfer processes. The available experimental data, however, are not yet sufficient to lead to a detailed understanding of the exciton migration mechanism and the mechanism of exciton trapping. Most recently Argyrakis and Kopelman [25] pointed out that it is unlikely that the diffusion model is an appropriate description due to the short lifetime of the singlet state, combined with the effectively two-dimensional exciton motion. They have investigated several types of random walk motion in a random binary lattice using the Monte Carlo technique [26]. Application of their results to the time dependence of the sensitized fluorescence yields preliminary results which are in fair agreement with the experimental observations [27]. This may indicate that the singlet-exciton motion in naphthalene is most adequately described as a two-dimensional "correlated hopping".

Regarding the temperature dependence of a/c_G (Fig. 14) it was noted in Ref. [22] that there is a reasonable agreement between the experimental results and the predictions given by Agranovich and Konobeev [28] on the basis of a partially coherent exciton motion. However, it should be pointed out that this is not the only model which predicts a temperature dependence of a/c_G which is reasonably close to the experimental observations.

In the following we will briefly discuss such a competing model, which is based on a simple hopping model. In order to account for the temperature dependence of the energy transfer rate one has to assume that the guest molecule is surrounded by perturbed host molecules, which act as primary shallow traps for the excitons [29, 30]. As soon as the exciton "falls" into such a localized state, it will be trapped in an energy funnel, in which it can only decay into states with lower energy and a greater degree of localization, except if thermal reactivation via exciton-phonon interaction takes place and promotes the exciton into energetically higher mobile states [31]. For simplicity it is assumed that the guest molecule is surrounded by a set of primary traps of trap depth ΔE and that thermal promotion into the band is unlikely once the exciton has reached the second step in the funnel. It is straightforward to show [32] that the rate of thermal promotion from the primary traps into the band, k_{up}, is related to the rate of transfer to the secondary trap, k_0, by the relation

$$k_{up} = k_0 \exp(-\Delta E/kT) . \tag{9}$$

As a consequence the total rate of energy transfer, predicted by this simple model, is given by

$$\begin{aligned} k_{HG}(T) &= a(T) \\ &= k_{HG}(0)[1 - \exp(-\Delta E/kT)] , \end{aligned} \tag{10}$$

where $k_{HG}(0)$, the rate of energy transfer at $T = 0$, is given by $k_0 c_T$. (c_T is the concentration of the primary traps.) In Fig. 15 this predicted behaviour is compared to the experimental results in a linear scale. The experimentally determined values of the quantity $k^0_{HG} = a/c_G$ are plotted as a function of the temperature. The full line was calculated by assuming that $k^0_{HG}(0) = 3.2 \times 10^{12}\ s^{-1}$ and $\Delta E = 18\ cm^{-1}$. Again the agreement between experimental results and the predictions of the model is fair, but it should be noted that the experimental data are not yet sufficient to make an unequivocal decision in favour of any particular model.

The assumption of a single trap depth ΔE for the primary traps is, of course, quite arbitrary and

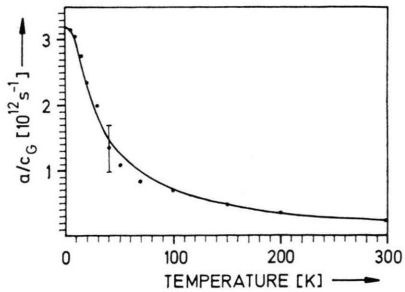

Fig. 15. Temperature dependence of $k^0_{HG} = a/c_G$ in a linear scale. The full line was calculated according to Eq. (10) using $k^0_{HG}(0) = 3.2 \times 10^{12}\ s^{-1}$ and $\Delta E = 18\ cm^{-1}$.

even unrealistic. But the fitting does not depend critically on the choice of ΔE and reasonable fits are obtained for $\Delta E \approx (22 \pm 10)$ cm^{-1}. It is reasonable to assume that ΔE is the "effective trap depth" of an ensemble of primary traps with trap depths within this range. By assuming particular distributions for these trap depths the fitting in Fig. 15 can be improved significantly. However, in the current state of affairs, the experimental data are not sufficient to make attempts to determine the trap distribution meaningful. But experiments with improved sensitivity and temporal resolution on additional systems will probably give a more profound insight into the physics of the energy-transfer process. Such experiments are currently under way.

It should be noted that the time-independent part of k_{HG} can also be determined from stationary experiments, since according to Eqs. (7) and (8) the stationary quantum flux ratio Q_G/Q_H of the guest and the host fluorescence at constant excitation is proportional to k_{HG}:

$$\frac{Q_G}{Q_H} = \frac{\eta_G}{\eta_H} \cdot \frac{k_{HG}}{k_H^0} \tag{11}$$

where η_G and η_H are the quantum yields of the guest and the host fluorescence, respectively. The temperature dependence of the quantum flux ratio has been determined by Hammer [33]. The resulting temperature dependence of $k_{HG}^0 = a/c_G$ is in agreement with that given in Figure 15.

A final remark should be added concerning the role of reabsorption in our experiments: Due to reabsorption processes the observed lifetime τ_H of the host fluorescence may be prolonged compared to the intrinsic lifetime τ_H^0 without reabsorption according to the following relation:

$$\tau_H = \tau_H^0/(1 - A\,\eta_H)\,, \tag{12}$$

where A is the reabsorption coefficient and η_H is the quantum yield of the host crystal. With $A = 0.7$ and $\eta_H = 0.175$ at $T = 300$ K [34] the effective increase of τ_H is roughly 12%, whereas at $T = 100$ K ($A = 0.12$, $\eta_H = 0.197$) the increase is only about 2%. Therefore in the evaluation of our experiments the influence of reabsorption has been neglected.

Acknowledgements

We are grateful to Professor H. C. Wolf for his interest in the progress in this work and the continuing support of it. Financial support by the Deutsche Forschungsgemeinschaft (Sonderforschungsbereich 67) is also gratefully acknowledged.

[1] S. Mansour and A. Weinreb, Chem. Phys. Letters **2**, 653 (1968).
[2] R. C. Powell and Z. G. Soos, J. Luminescence **11**, 1 (1975). References to the extensive work of Powell and coworkers are compiled in this review.
[3] R. C. Powell and Z. G. Soos, Phys. Rev. **B 5**, 1547 (1972).
[4] Z. G. Soos, and R. C. Powell, Phys. Rev. **B 6**, 4035 (1972).
[5] J. A. Giordmaine, P. M. Rentzepis, S. L. Shapiro, and K. W. Wecht, Appl. Phys. Letters **11**, 216 (1967).
[6] A. Hammer, Dissertation, Universität Stuttgart 1968.
[7] G. Zibold, Diplomarbeit, Universität Stuttgart 1968.
[8] A. Bergman, D. Bergman, and J. Jortner, Israel J. Chem. **10**, 471 (1972).
[9] F. Heisel, J. A. Miehe, B. Sipp, and M. Schott, Chem. Phys. Letters **43**, 534 (1976).
[10] A. J. Campillo, R. C. Hyer, S. L. Shapiro, and C. E. Swenberg, Chem. Phys. Letters **48**, 495 (1977).
[11] F. Heisel, J. A. Miehe, B. Sipp, and M. Schott, Chem. Phys. Letters **56**, 178 (1978).
[12] H. Auweter, U. Mayer, and D. Schmid, Z. Naturforsch. **33a**, 651 (1978).
[13] H. C. Wolf, Festkörperprobleme **4**, 57 (1965).
[14] A. Bree and T. Thirunamachandran, Mol. Phys. **5**, 397 (1962).
[15] U. Gösele, Chem. Phys. Letters **43**, 61 (1976).
[16] M. Grover and R. Silbey, J. Chem. Phys. **54**, 4843 (1971).
[17] R. M. Hochstrasser and J. E. Wessel, Chem. Phys. Letters **24**, 1 (1974).
[18] R. M. Hochstrasser, H. N. Sung, and J. E. Wessel Chem. Phys. Letters **24**, 168 (1974).
[19] A. Bergman and J. Jortner, Chem. Phys. Letters **26**, 323 (1974).
[20] V. A. Benderskii, V. KH. Brikenstein, A. G. Lavrushko, P. G. Filipov, and A. V. Yatsenko, Chem. Phys. Letters **56**, 443 (1978).
[21] M. Köhler, D. Schmid, and H. C. Wolf, J. Luminescence **14**, 41 (1976).
[22] A. Braun, H. Pfisterer, and D. Schmid, J. Luminescence **17**, 15 (1978).
[23] S. Chandrasekhar, Rev. Mod. Phys. **15**, 1 (1943).
[24] J. Heber, Phys. Stat. Sol. (b) **48**, 319 (1971).
[25] P. Argyrakis and R. Kopelman, Chem. Phys. Letters **61**, 187 (1979).
[26] P. Argyrakis and R. Kopelman, J. Theor. Biol. **73**, 205 (1978).
[27] R. Kopelman, private communication.
[28] V. M. Agranovich and Y. V. Konobeev, Phys. Stat. Sol. **27**, 435 (1968).
[29] D. P. Craig and M. R. Philpott, Proc. Roy. Soc. London A **290**, 583 (1966).
[30] D. P. Craig and M. R. Philpott, Proc. Roy. Soc. London A 293, 213 (1966).
[31] M. D. Fayer and C. B. Harris, Phys. Rev. **B 9**, 748 (1974).
[32] B. di Bartolo, Optical Interactions in Solids, John Wiley & Sons, Inc. New York 1968, p. 341.
[33] A. Hammer and H. C. Wolf, Mol. Cryst. **4**, 191 (1968).
[34] A. Hammer and H. C. Wolf, Phys. Stat. Sol. **33**, K 25 (1969).